

Data-driven Optimization for Underactuated Robotic Hands

Matei Ciocarlie and Peter Allen

Abstract—Passively adaptive and underactuated robotic hands have shown the potential to achieve reliable grasping in unstructured environments without expensive mechanisms or sensors. Instead of complex run-time algorithms, such hands use design-time analysis to improve performance for a wide range of tasks. Along these directions, we present an optimization framework for underactuated compliant hands. Our approach uses a pre-defined set of grasps in a quasistatic equilibrium formulation to compute the actuation mechanism design parameters that provide optimal performance. We apply our method to a class of tendon-actuated hands; for the simplified design of a two-fingered gripper, we show how a global optimum for the design optimization problem can be computed. We have implemented the results of this analysis in the construction of a gripper prototype, capable of a wide range of grasping tasks over a variety of objects.

I. INTRODUCTION AND RELATED WORK

In recent years, research on robotic grasping has focused increasing attention on passively adaptive hands. Such designs are usually defined as having the ability to passively comply to the shape of a grasped object, at a mechanical rather than computational level. As a result, they require less complex control algorithms, which in turn reduces the need for extensive sensing capabilities and increases reliability in unstructured environments. Furthermore, since fine posture adjustments are performed through passive compliance, a mechanically adaptive hand can afford to use fewer actuators than a non-adaptive model. The combination of mechanical adaptation and underactuation promises to result in robotic hands that are effective even in the presence of sensing errors, while maintaining a low production cost and enabling fast design iterations.

It is very important to note, however, that this extensive set of useful features does not come for free. Truly reliable performance in a wide range of grasping tasks requires careful optimization of the hand design parameters. In a sense, on-line sensing and computation efforts specific to a particular grasp must be replaced by off-line analysis and optimization, carried out before the hand is even built, in order to ensure positive outcomes for an entire range of tasks. Interestingly, the results of this optimization effort are easiest to overlook when it is most successful, and produces a deceptively simple yet highly efficient hand.

There are multiple ways of achieving passive adaptation with a robotic hand design. Perhaps the earliest example is the Soft Gripper introduced by Hirose and Umetani [1], using tendons for both flexion and extension. Ulrich et al. [2]

pioneered the use of a breakaway transmission mechanism which is now used in the Barrett hand (Barrett Technologies, Cambridge, MA). Dollar and Howe [3] optimized the actuation and compliance forces of a single tendon design with spring-like joints providing extension forces, which they later implemented in the Harvard Hand [4]. Gosselin et al. [5] also proposed a tendon-driven design for a robotic hand with 15 degrees of freedom and a single actuator.

Birglen et al. [6] presented a detailed and encompassing optimization study for underactuated hands, focusing mainly on four-bar linkages but with applications to other transmission mechanisms as well. Four-bar linkages were also used to construct the MARS hand [7], which later evolved into the SARAH family of hands [8]. These studies have led to the construction of remarkably efficient grippers and hands. In the process, they have also highlighted the fact that optimization of a highly underactuated hand is a complex problem; in other words, *simple is hard!*

An important body of work has also focused on the force generation capabilities of redundant or tendon-driven mechanisms in the context of studying the human hand. Relevant examples include [9]–[12]. Highly underactuated anthropomorphic hand models include the work of Brown and Asada [13] and Carrozza et al. [14]; the latter also makes use of the principles of passive adaptation. Finally, force generation has been studied extensively in the context of fully actuated robotic hands, and a number of useful tools have been proposed; see [15]–[18] and references therein for details. However, the combination of highly underactuated and adaptive grasping present a number of additional challenges, some of which we attempt to tackle in this study.

II. A FRAMEWORK FOR UNDERACTUATED HAND OPTIMIZATION

In our own previous work [19], which we will briefly review in the next section, we have introduced a set of tools for performing underactuated grasp analysis. In this paper, we extend and apply those tools as part of an optimization framework for a class of underactuated adaptive hands. The methods presented here integrate the following main stages:

- we start from a given kinematic design, with a palm and multiple fingers, yielding a potentially large number of joints;
- assuming that each joint can be controlled independently, we create a set of stable grasps over a given group of objects. We refer to this set as the *optimization pool*;
- we extend our previous work on underactuated grasp analysis to consider an entire set grasps (rather than one

This work was funded in part by NIH BRP grant 1R01 NS 050256-01A2
All authors are with the Dept. of Computer Science, Columbia University, NY, USA. E-mail: {cmatei, allen}@cs.columbia.edu

- grasp at a time) and make the hand actuation parameters the optimized variables;
- we optimize the parameters of the underactuation mechanism such that it provides the best performance for the hand over the entire pool of grasps, taking into account the constraints of joint co-actuation and passive adaptation;
 - for a particular class of robotic grippers, this optimization problem can be cast in a form for which efficient algorithms exist that can compute a global optimum (such as a Linear or Quadratic Program). For this case, we build and demonstrate a proof-of-concept prototype. We also discuss an extension to more complex designs, which suggest the use of numerical, gradient-based optimization methods.

We have already noted that the passive adaptation concept can be implemented in hardware using multiple actuation methods; the choice of which method to use is one of the first decisions to be made when starting the design of a passively compliant hand. In this paper, we construct our framework using the mechanics of a tendon-actuated hand combined with compliant, spring-like joints. This allows us to provide a concrete example and implementation of the optimization results. However, other actuation methods can be considered in future iterations.

Our method is general, in the sense that, for the pool of desired grasps that drives the optimization process, it can accept arbitrary 3D object geometry and takes into account contact frictional constraints. However, the most general case, which also accepts arbitrary hand kinematics, exhibits a number of non-linearities that prevent a global solution. Conversely, the simpler and more constrained case of a two-fingered gripper with a single tendon allows fast computation of a provable global optimum. We will discuss both cases in detail in the following sections.

III. PROBLEM FORMULATION

The starting point for our optimization framework is the quasistatic equilibrium relationship that characterizes a stable grasp. We briefly review this formulation here; for more details and applications we refer the reader to the analysis by Prattichizzo and Trinkle [20] as well as our previous study [19].

Consider a grasp with p contacts established between the hand and the target object. For any contact i , the total contact wrench c_i must obey two constraints. First, the normal component must be positive (contacts can only push, not pull). Second, friction constraints must be obeyed. A common method is to linearize these constraints, by expressing c_i as a linear combination of normal force and possible friction wrenches. The complete contact constraints are:

$$c_i = D_i \beta_i \quad (1)$$

$$\beta_i, F_i \beta_i \geq 0 \quad (2)$$

where the matrices D_i and F_i depend only on the chosen friction model, such as linearized Coulomb friction (more

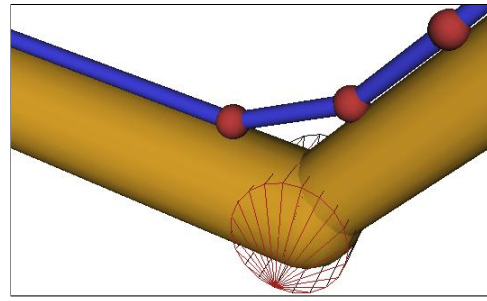


Fig. 1. Illustration of tendon routing points, marked with red spheres, as the tendon follows a revolute joint marked by a wire frame cylinder.

details on the construction of these matrices can be found in [19], [21]). The contact wrench is now completely determined by the vector of friction and normal wrench amplitudes β_i , which will be computed as part of the grasp analysis algorithm.

We can now move on to the analysis of the complete grasp, as a collection of multiple contacts. In general, a grasp is in equilibrium if the following conditions are satisfied:

- contact forces are balanced by joint forces (hand is in equilibrium);
- resultant object wrench is null (object is in equilibrium);
- contact constraints are met for all contacts that constitute the grasp.

We can assemble this grasp description as follows:

$$J_c^T D \beta = \tau \quad (3)$$

$$G \beta = 0 \quad (4)$$

$$\beta, F \beta \geq 0 \quad (5)$$

where τ is the vector of joint forces, J_c is the Jacobian of the contact locations and G is the grasp map matrix that relates individual contact wrenches to the resultant object wrench. The matrices D and F bring together the individual contact constraint matrices D_i and F_i for $i = 1 \dots p$ in block diagonal form. The column vector β contains all contact amplitudes vectors β_i in block column form. Finally, in order to avoid the trivial solution where all forces in the system are zero, an additional constraint can be added requiring total actuator forces to sum to a pre-specified level.

In this paper, we use the term “stable” to refer to grasps that are in quasistatic equilibrium (all of the above constraints are met). In practice, this is not a sufficient condition for achieving form-closure using the given actuation mechanism. However, it is a necessary prerequisite and, as such, we believe that optimizing a hand to achieve equilibrium under many configurations is a valuable step towards enabling a wide range of grasps. A possible future extension would be to also include a direct measure of grasp quality, according to one of the metrics that have been proposed in the literature. One possibility (as derived, for example, by Prattichizzo and Trinkle [20]), would be to not only constrain contact forces to satisfy their friction constraints, but also optimize them to be as far from the boundaries of acceptable values as possible.

So far, this analysis applies to a hand design regardless of its actuation method. To adapt it to the case of underactuated hands, we must look in more detail at the joint force vector τ , which is a result of the actuation mechanism. In this paper, we chose to focus on an actuation method that combines tendons and spring-like compliant joints. We use the common tendon-pulley model (as used for example by Kwak et al. [22]), which assumes that the tendon travels through a number of routing points that it can slide through, but which force it to change direction as it follows the kinematic structure. As a result of this change in direction, the routing points are the locations where the tendon applies force to the links of the finger. This model is illustrated in Fig. 1, with the routing points marked with spheres. For clarity, the route shown is on the surface of the links, but in general the tendon can also be tunneled through the inside of the links.

We assume that the hand contains a total of d tendons, each with multiple routing points across different links. In this case, joint forces can be expressed as:

$$\tau = \mathbf{J}_d^T \delta + \theta \mathbf{k} \quad (6)$$

where \mathbf{J}_d is the Jacobian of the tendon routing points and $\delta \in \mathcal{R}^d$ is the vector of applied tendon forces. θ is a diagonal matrix of joint angle values and \mathbf{k} is the vector of joint spring stiffnesses (without loss of generality, we assume 0 is the rest position for all springs). We now have a complete description of the equilibrium state of the grasp, expressed in eqs. (3) through (6).

It is important to note that not all grasps, and not all hand actuation mechanisms, allow all of the above conditions to be met. In such cases, we can still use this formulation by turning one of the conditions into an optimization objective, rather than a hard constraint, as we describe next.

A. Grasp Analysis

Consider first the simpler application of grasp analysis. Here, we assume that the hand structure and actuation are set; the goal is to analyze a given grasp, determine if it is stable and assign it a numerical quality metric. In other words, the goal is to determine the contact forces β and actuation forces δ that satisfy our formulation, or, if exact equilibrium is not feasible, come as close as possible:

$$\begin{aligned} \text{minimize } \|\mathbf{G}\beta\| &= \beta^T \mathbf{G}^T \mathbf{G} \beta \quad \text{subject to :} \\ \mathbf{J}_c^T \mathbf{D}\beta - \mathbf{J}_d^T \delta &= \theta \mathbf{k} \end{aligned} \quad (7)$$

$$\delta, \beta, \mathbf{F}\beta \geq 0 \quad (8)$$

This is a standard Quadratic Program with linear constraints. Furthermore, the quadratic objective matrix is positive semidefinite; therefore, the problem is convex and a global optimum can be determined. The result is the lowest magnitude unbalanced wrench that the grasp applies on the object, which provides us with a measure for the quality of the grasp. If its magnitude is exactly 0, the grasp is stable in the current configuration. If not, some level of unbalanced force is applied to the object, which either must be supported externally (e.g. through other contacts with the environment) or will require a reconfiguration of the hand-object system.

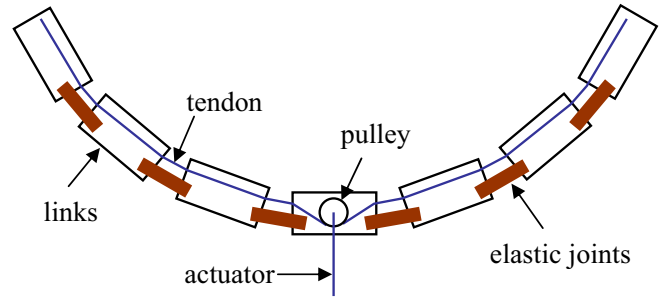


Fig. 2. Design of a two-fingered gripper with single tendon actuation used as a case study for the optimization framework.

B. Hand Optimization

The next application that we present is also the main focus of our paper: optimization of the hand actuation mechanism to obtain best performance over a given set of desired grasps. The goal is to compute both contact and actuation forces (as above), which are specific to each grasp, and actuation parameters, which are shared between all the grasps, in order to ensure the most stable results over all the grasps in the optimized set. In particular, we would like to compute the optimal values for both the locations of the tendon routing points and the stiffnesses of the joint springs. The latter is relatively straightforward, as we can simply add the vector \mathbf{k} to the list of unknowns. Tendon routing however presents additional challenges.

One possible approach is to optimize the location of the routing points (and thus the tendon route) on their respective links. The effects of the tendon route on the equilibrium condition are encapsulated in the Jacobian of the routing points, \mathbf{J}_d . However, changing the location of a routing point on a link has a highly non-linear effect on \mathbf{J}_d . Furthermore, even if we had a linear relationship between the tendon route parameters and the routing point Jacobian, the result must then be multiplied by the unknown vector of actuation forces δ . Computing both actuation forces and optimal tendon route parameters at the same time results in a higher order equality constraint which can not be handled by the same optimization tools.

The general case therefore enables us to quantify a given actuation mechanism (by computing the quality of each grasp in the optimization pool), but not to directly compute its global optimum. We envision two possible solutions to this problem. The first one is to perform numerical optimization instead, either through numerical computation of a gradient or through other algorithms such as simulated annealing. The second option is to use a simplified, more constrained formulation, which accepts a provable global optimum to the tendon route optimization problem. We explore this approach in detail in the following sections.

IV. CASE STUDY: SINGLE-TENDON GRIPPER

As a testbed for our optimization framework, we use the two finger model (which we will refer to as a gripper, rather than a hand) presented in Fig. 2. A single tendon provides

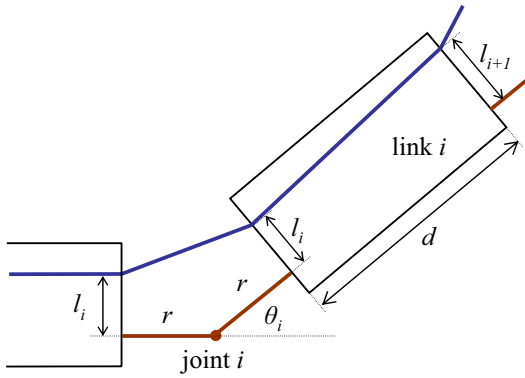


Fig. 3. Detailed description for a joint of the proposed gripper design.

flexion forces for both fingers, which are co-actuated using a pulley mechanism, similar to the one used in the Harvard Hand [4]. Note that the pulley allows one finger to continue flexing even if the other finger is blocked by contact with the object. Extension forces are provided by using spring-like joints. In practice, these joints can be constructed using a compliant, rubber-like material; this design enables distal joints to flex even when proximal joints are stopped, also providing mechanical adaptability. We assume that the kinematic behavior is that of ideal revolute joints, with the center of rotation placed halfway between the connected links.

The tendon itself follows a route in the flexion-extension plane of the gripper. This prevents the links from leaving this plane without the application of external forces, leading to an essentially two-dimensional design. However, the tendon route inside this plane is not specified, and is one of the targets of the optimizations.

Fig. 3 shows in detail the design parameters of the gripper. The tendon route is determined by the location of the entry and exit points for each link; more specifically, the parameter that we use is the distance between the tendon entry or exit point and the connection between the link and the joint. We also make the simplifying assumption that, for a joint i , the exit point from the proximal link and the entry point in the distal link have the same value for this parameter, which we call l_i . The current value of the joint is θ_i . r is the joint radius (shared by all the joints), while the length of the links is denoted by d .

The reason for using this design and formulation is that they yield a compact and, more importantly, linear relationship between the construction parameters and the joint forces applied through the tendon. If we consider the parameter vector $\mathbf{p} = [l_0 \ l_1 \ l_2 \ l_3 \ l_4 \ l_5 \ r \ d]$, we obtain a relationship of the form:

$$\boldsymbol{\tau} = \boldsymbol{\delta}(\mathbf{B}\mathbf{p} + \mathbf{a}) + \boldsymbol{\theta}\mathbf{k} \quad (9)$$

where the matrix $\mathbf{B} \in \mathcal{R}^{8 \times 8}$ and the vector $\mathbf{a} \in \mathcal{R}^8$ depend only on the joint values $\theta_0 \dots \theta_5$. A sketch for the derivation of these matrices is presented in the Appendix.

Furthermore, since we are using a single tendon, $\boldsymbol{\delta} \in \mathcal{R}$. Without loss of generality, we can normalize its value to

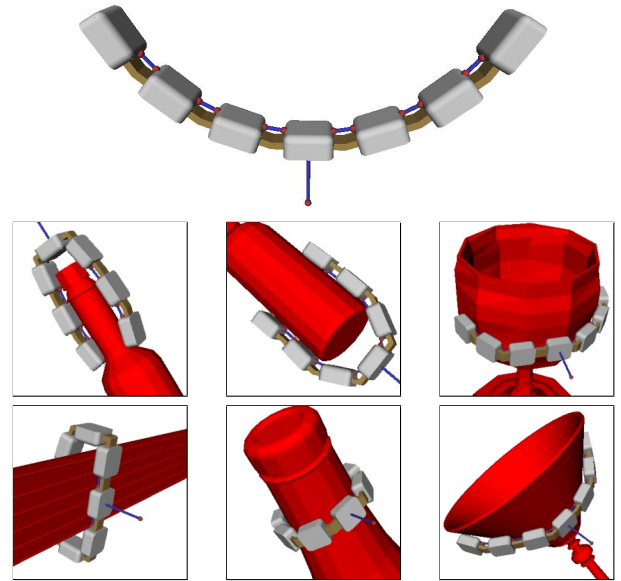


Fig. 4. Top: gripper model for the *GraspIt!* environment. Bottom: examples of grasps from the optimization pool.

$\delta = 1$. The joint force relationship, and by extension the grasp equilibrium conditions, are now fully linear, in all of the unknowns.

A. Optimization pool

Having established the general characteristics of the gripper, the next step was to generate a pool of grasps over which to optimize its performance. To this end, we used the publicly available *GraspIt!* simulator [23], previously developed in the Columbia Robotics Lab.

We first created a kinematic model of the gripper for the *GraspIt!* environment, assuming each joint could be controlled independently. Then, using the interaction tools in the simulator, we manually specified a number of grasp postures over a set of 3D models of common household objects. The set comprised 70 grasps distributed across 15 objects; the process is illustrated in Fig. 4. Each grasp was defined by the set of gripper joint angles, the location of the contacts on each link, and the contact surface normals. We note that this is a purely “geometric” description of a grasp, with no reference to the actuation mechanism.

Most of the grasps in the pool used different postures for the two fingers of the gripper. We thus added to the set the “transpose” of each grasp, obtained by rotating the gripper by 180 degrees around the wrist roll axis, essentially reversing the roles of the left and right finger. The complete optimization pool thus comprised 140 grasps. The inclusion of both the original and the transposed grasps also ensured that the final optimized parameters, presented in the next section, were symmetrical, with identical results for both fingers.

A key restriction during the creation of the optimization pool was that all the grasps therein were required to have form-closure. *GraspIt!* integrates a number of analysis tools for establishing the form-closure property by build-

ing the Grasp Wrench Space, as described by Ferrari and Canny [24]. This formulation is equivalent to the ability of a set of contacts to apply a null resulting wrench on the object while satisfying contact friction constraints, but disregarding any kinematic or actuation constraints. The contact friction model that we used was a linearized version of the Soft Finger model which we presented in previous work [25]. This enabled us to simulate links coated in a layer of soft rubber, providing local compliance at the point of contact and allowing frictional torque.

We note that using a pre-defined grasp optimization pool also restricts the set of parameters that can be part of the optimization. In particular, changing the values of parameters r (joint radius) and d (link length) would require a new set of grasps to reflect the changed kinematics of the hand. In this study, we fixed the values of r and d and focused on the parameters l_i and k_i , which are specific to the actuation mechanism. One possible way to alleviate this constraint is to generate the optimization pool automatically for any given set of kinematic parameters; we will further investigate this possibility in our future work.

B. Complete Optimization Problem

For each grasp in our optimization pool, we can apply the equilibrium formulation from section III, using the actuation mechanism modeled as described earlier in this section. The complete relationship is

$$(\mathbf{J}_c^j)^T \mathbf{D}^j \boldsymbol{\beta}^j = \mathbf{B}^j \mathbf{p} + \mathbf{a}^j + \boldsymbol{\theta}^j \mathbf{k} \quad (10)$$

$$\mathbf{G}^j \boldsymbol{\beta}^j = 0 \quad (11)$$

$$\boldsymbol{\beta}^j, \mathbf{F}^j \boldsymbol{\beta}^j \geq 0 \quad (12)$$

where we use the superscript j to denote the index number of the particular grasp from the optimization pool that we are referring to. The unknowns are the grasp contact forces $\boldsymbol{\beta}^j$, the hand parameter vector \mathbf{p} , and the vector of joint spring stiffnesses \mathbf{k} . Note that \mathbf{p} and \mathbf{k} do not have a superscript as they are shared between all the grasps in the pool.

To obtain a global optimization problem, we assemble the above relationships in block form over the entire pool containing a total number of g grasps. The matrices for individual grasps $(\mathbf{J}_c^j)^T \mathbf{D}^j$, \mathbf{B}^j , $\boldsymbol{\theta}^j$, \mathbf{G}^j and \mathbf{F}^j are assembled in block diagonal form for $j = 1 \dots g$ in the matrices $\tilde{\mathbf{J}}_c^T \tilde{\mathbf{D}}$, $\tilde{\mathbf{B}}$, $\tilde{\boldsymbol{\theta}}$, $\tilde{\mathbf{G}}$ and $\tilde{\mathbf{F}}$, respectively. The vectors $\boldsymbol{\beta}^j$ and \mathbf{a}^j are assembled in block columns in the vectors $\tilde{\boldsymbol{\beta}}$ and $\tilde{\mathbf{a}}$. Finally, the joint equilibrium condition (10) assembled for all the grasps in the pool becomes the optimization objective.

$$\text{minimize} \quad \left\| \left[\tilde{\mathbf{J}}_c^T \tilde{\mathbf{D}} - \tilde{\mathbf{B}} - \tilde{\boldsymbol{\theta}} \right] \begin{bmatrix} \tilde{\boldsymbol{\beta}} \\ \mathbf{p} \\ \mathbf{k} \end{bmatrix} - \tilde{\mathbf{a}} \right\| \quad \text{subject to:}$$

$$\tilde{\mathbf{G}} \tilde{\boldsymbol{\beta}} = 0 \quad (13)$$

$$\tilde{\boldsymbol{\beta}}, \tilde{\mathbf{F}} \tilde{\boldsymbol{\beta}} \geq 0 \quad (14)$$

$$\mathbf{p}_{min} \leq \mathbf{p} \leq \mathbf{p}_{max} \quad (15)$$

$$\mathbf{k}_{min} \leq \mathbf{k} \leq \mathbf{k}_{max} \quad (16)$$

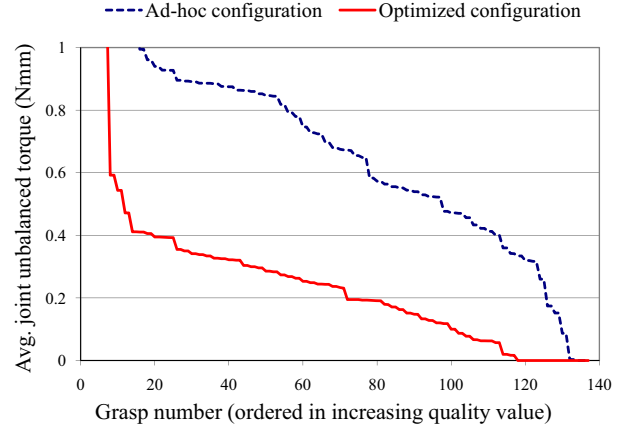


Fig. 5. Comparison of unbalanced joint forces as a measure of grasp stability between optimized and ad-hoc configuration

Parameter	l_o	l_1	l_2	k_o	k_1	k_2
Optimized value	5.0	5.0	1.72	1.0	1.0	2.0

TABLE I

RESULTS OF GRIPPER DESIGN OPTIMIZATION

The minimum and maximum values for the construction parameters \mathbf{p} and \mathbf{k} can be set to reflect constraints in the physical construction of the gripper, as we will show in the applied example in the next section.

We note that the result is also a convex Quadratic Program. Furthermore, the program is always feasible by construction: constraints (13) and (14) are equivalent to each individual grasp having form-closure independently of the actuation mechanism, which we ensured by building our grasp pool accordingly. As a result, the problem can always be solved and a global optimum can be computed.

V. IMPLEMENTATION AND RESULTS

The final step of using our framework was physical construction of a gripper according to the results of the optimization. This required limits for the optimized parameters that could be implemented in practice. In particular, we used a limit of $-5mm \leq l_i \leq 5mm \forall i$ to ensure that the tendon route was inside the physical volume of each link. We also used values of $r = 5mm$ and $d = 20mm$ for the kinematic parameters that were not included in the optimization.

The joint stiffness levels require additional discussion. The first thing to note is that the deciding factors for the behavior of the hand are the relative ratios of individual joint stiffnesses, not their absolute values. Indeed, increasing all stiffness values by a constant factor only scales all the forces in the system accordingly, without a qualitative change in the result. In practice, this would suggest using the lowest absolute values that yield the desired ratios, as this would have the effect of scaling down the level of unbalanced forces applied to the object. However, when using fast construction methods and inexpensive materials, very low, yet reliable

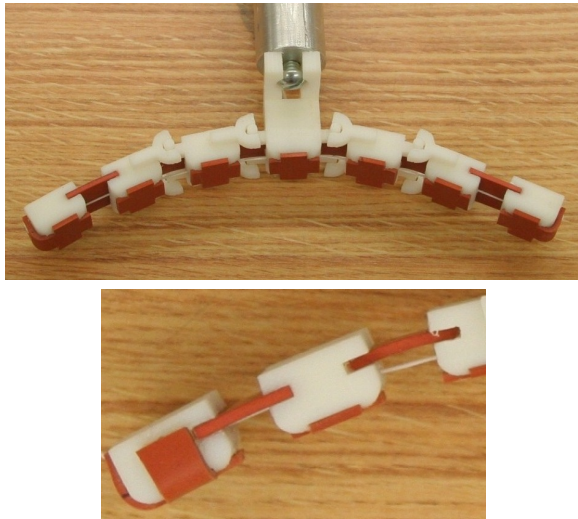


Fig. 6. Prototype gripper constructed according to optimization results. Notice the different tendon route and rubber joint dimensions between the two distal joints.

stiffness values are hard to implement; so are very large relative ratios. In practice, we used as limits $1.0 \leq k_i \leq 2.0$. However, these limits can always be adapted based on the available materials and construction methods.

The results of the optimization are shown in Table I. We only show the values for one of the fingers, since, as mentioned before, the results for the other finger are symmetrical. For a quantitative analysis of the computed optimal configuration, we compared it against a gripper configuration using an ad-hoc parameter set, with $l_i = 5$ and $k_i = 1 \forall i$. The comparison criterion was the level of unbalanced joint forces for each grasp. The results are shown in Fig. 5. We notice that the optimized configuration provides significantly more stable grasps across the optimization pool. The total time spent formulating and solving the optimization problem was less than a minute, using a commodity desktop computer equipped with a 2.4GHz Intel Core2 Duo CPU. This suggests the future possibility of scaling to much larger grasp optimization pools.

A. Gripper Construction and Grasping Results

We constructed a prototype gripper using the results of the optimization. The links were built using a Stratasys FDM rapid prototyping machine, and assembled using elastic joints cut from a sheet of hard rubber. Each link contained a tendon route with the entry and exit points set according to the optimization results. The width of the strip of rubber was varied for each joint to provide the specified stiffness ratios. For the tendon we used kite wire, which provided the desired combination of strength, flexibility and low friction. As this prototype is intended as a proof-of-concept for the kinematic configuration and design parameters, no motor or sensors were installed. Instead, actuation was performed manually. The final result is shown in Fig. 6.

We found that the prototype gripper is capable of a wide range of grasping tasks and does not require precise

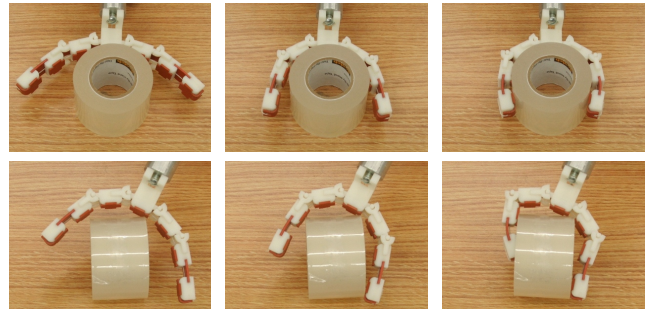


Fig. 7. Two grasps executed with the prototype gripper. Top row: centered starting position and symmetrical grasp. Bottom row: off-centered starting position requiring passive adaptation to an irregular shape.

positioning relative to the target object. Its passive adaptation ability is exemplified in Fig. 7, which shows the execution of two grasps. The first one starts from a centered position and leads to relatively similar joint values for both fingers. In contrast, the second grasp requires the joints to conform to an asymmetrical, irregular shape. Both grasps were executed successfully.

Figure 8 attempts to provide an illustration of the spectrum of grasps that can be carried out with this gripper. All of the presented grasps were executed successfully and the object was securely lifted off the table, with very little time or effort spent positioning the gripper relative to the target. In particular, we note that the gripper is capable of executing both fingertip grasps (of varying finger spans) and enveloping grasps (of both regular and irregular shapes).

B. Discussion

Starting from the observation that our grasp examples (as well as the optimization pool) contain both fingertip and enveloping grasps, we can attempt to perform a qualitative analysis of the optimization results. Intuitively, fingertip grasps require relatively low torques on the distal joints, so that fingertip forces are in opposition, rather than oriented towards the palm. Conversely, larger torques on the distal joints benefit enveloping grasps; as a result, the optimization process was required to combine two somewhat opposing goals. The results indicate that the solution does indeed enable both kinds of grasps, however the distal joint is both stiffer and less powerful than the proximal ones. In fact, our optimization framework achieves this characteristic by “saturating” many of the hand parameters, which take either the minimum or maximum value allowed.

It is interesting to note that, in this sense, the result of the optimization could be interpreted as meaning that the addition of a third link to the gripper provides little benefit. The resulting gripper comes close to a model with two links per finger, a design also confirmed in the optimization studies of Dollar and Howe [3]. We believe that this is precisely the type of analysis that our framework is natively well suited for. In future iterations, we can directly compare two- versus three-link models, and compute a *numerical measure* of the benefit provided by the additional link. The relatively simple two-fingered design that we used here allows an intuitive

understanding of the design choices (which makes it well suited for initial testing and proof-of-concept implementations). However, for more complex models with multiple fingers, such qualitative analysis quickly becomes intractable, and quantitative tools, such as the one presented here, can prove extremely valuable.

VI. CONCLUSION AND FUTURE WORK

In this paper we have focused on the problem of optimizing underactuated and passively adaptive robotic hands. For designs belonging to this class, the ability to apply forces to a grasped object is affected by co-actuation constraints. We have integrated these constraints in a quasistatic equilibrium formulation, also taking into account contact friction models. For a particular class of hands, constructed using tendons and spring-like joints, we have shown how this formulation allows a direct analysis of the quality of an underactuated grasp. We have also presented a simplified design, using a two-fingered kinematic mechanism actuated via a single tendon. Using this model, we can build a solvable optimization problem to compute the design parameters that provide the best performance over a large set of grasping tasks. We have demonstrated this behavior both in simulation and by constructing a gripper prototype.

We have identified two possible cases for framing hand design decisions as optimization problems. One one hand, adding a number of design constraints (as in the case of our gripper) enables the direct computation of a global optimum. This is the option that we have explored in detail in this study. On the other hand, for the more general problem, a number of non-linearities in the formulation prevent a similar solving strategy. Instead, more expensive, iterative algorithms could be employed. In our future work, we intend to implement such a solver for more general hand designs, and further explore the interplay between additional constraints and the optimization advantages that they afford.

Another interesting extension regards the set of grasps used as an optimization pool. In our current implementation, this set was generated manually, which prevented complete automation of the optimization process. This can be replaced by an automated search procedure, running in a simulated environment, which can generate and analyze the pool of desired grasps. Such a complete procedure would enable many kinematic designs to be tested without human attention, allowing us to use more computational resources for exploring the space of possible robotic hand designs.

Finally, we must also keep in sight our main goal, of applying optimized hand designs to tasks in unstructured settings. One possible direction is to add motor and sensing capabilities to the gripper model that we have introduced, in order to test its abilities when using autonomous grasping strategies. We believe that research on adaptive and underactuated designs can ultimately provide us with inexpensive and easy-to-build, yet effective robotic hands for a variety of applications in human environments.

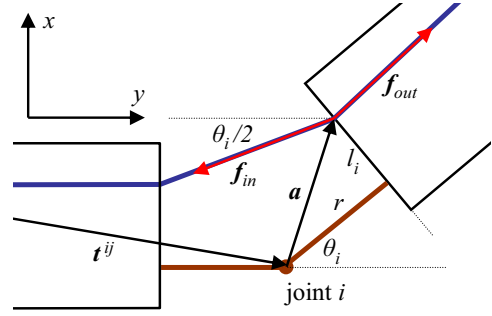


Fig. 9. Torque computation for tendon entry point

APPENDIX

In order to sketch the derivation for the relationship between the tendon route parameters and the resulting joint torques, we start by focusing on how tendon entry and exit points on link i affect the torque applied at joint j . Using the notation shown in Fig. 9, we use joint i as our reference coordinate frame, and assume that the translation from joint j to joint i is $\mathbf{t}^{ij} = [t_x^{ij} \ t_y^{ij}]^T$.

In general, for any point where a tendon changes direction, such as the link entry point in the figure, the force applied to the link is the resultant of the total tendon force applied in both the initial and the changed direction, or $\mathbf{f} = \mathbf{f}_{in} + \mathbf{f}_{out}$. We note that $\|\mathbf{f}_{in}\| = \|\mathbf{f}_{out}\| = \delta$. However, since we normalize tendon force to $\delta = 1$ we can omit it from the computations. We then obtain the torque applied around a given joint by cross-product with the joint moment arm. Using this notation, the torque around joint j applied at the tendon entry point in link i is:

$$\begin{aligned} \tau_{\text{entry}}^{ij} &= (\mathbf{t}^{ij} + \mathbf{a}) \times (\mathbf{f}_{in} + \mathbf{f}_{out}) \quad (17) \\ &= \left(\begin{bmatrix} t_x^{ij} \\ t_y^{ij} \end{bmatrix} + \begin{bmatrix} \cos\theta_i & \sin\theta_i \\ -\sin\theta_i & \cos\theta_i \end{bmatrix} \begin{bmatrix} l_i \\ r \end{bmatrix} \right) \times \\ &\quad \times \left(\begin{bmatrix} -\sin(\theta_i/2) \\ -\cos(\theta_i/2) \end{bmatrix} + \begin{bmatrix} \sin\theta_i \\ \cos\theta_i \end{bmatrix} \right) \quad (18) \end{aligned}$$

Through a similar computation, using the notation from Figs. 3 and 9, we can compute the torque applied at the tendon exit point from link i as:

$$\begin{aligned} \tau_{\text{exit}}^{ij} &= \left(\begin{bmatrix} t_x^{ij} \\ t_y^{ij} \end{bmatrix} + \begin{bmatrix} \cos\theta_i & \sin\theta_i \\ -\sin\theta_i & \cos\theta_i \end{bmatrix} \begin{bmatrix} l_{i+1} \\ r + d \end{bmatrix} \right) \times \\ &\quad \times \left(\begin{bmatrix} \sin(\theta_i + \theta_{i+1}/2) \\ \cos(\theta_i + \theta_{i+1}/2) \end{bmatrix} + \begin{bmatrix} -\sin\theta_i \\ -\cos\theta_i \end{bmatrix} \right) \quad (19) \end{aligned}$$

If $l_i \neq l_{i+1}$, the tendon must also change direction somewhere inside link i . The resulting torque is simply:

$$\tau_{\text{change}}^{ij} = l_{i+1} - l_i \quad (20)$$

All of these contributions are added to obtain the total torque applied on joint j due to tendon routing points on link i . Finally, the computation above is repeated for all desired combinations of i and j . By explicitly computing cross products as $\mathbf{u} \times \mathbf{v} = [v_y \ -v_x][u_x \ u_y]^T$ we obtain the

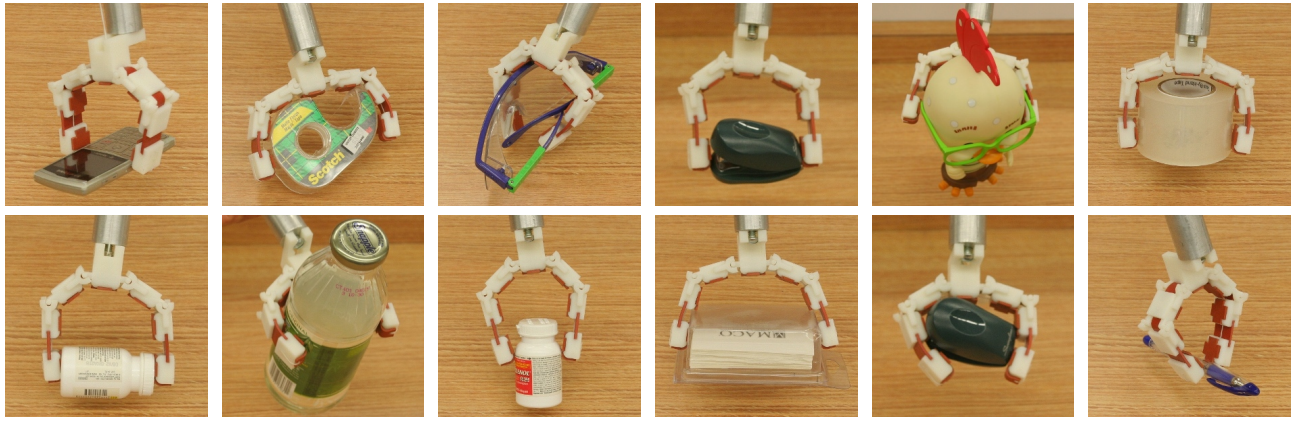


Fig. 8. An example set of grasps successfully executed using the prototype gripper.

respective entries in the matrix B and the vector α , which are then assembled in the linear relationship

$$\tau_{\text{tendon}} = B(\theta)p + \alpha(\theta) \quad (21)$$

which can then be integrated in the complete grasp formulation presented in the paper.

REFERENCES

- [1] S. Hirose and Y. Umetani, "The development of soft gripper for the versatile robot hand," *Mechanism and Machine Theory*, vol. 13, pp. 351–358, 1978.
- [2] N. Ulrich, R. Paul, and R. Bajcsy, "A medium-complexity compliant end effector," in *IEEE International Conference on Robotics and Automation*, 1988, pp. 434–439.
- [3] A. Dollar and R. Howe, "Joint coupling design of underactuated grippers," in *30th Annual Mechanisms and Robotics Conference*, September 2006.
- [4] A. Dollar and R. Howe, "Simple, robust autonomous grasping in unstructured environments," in *IEEE International Conference on Robotics and Automation*, 2007, pp. 4693–4700.
- [5] C. Gosselin, F. Pelletier, and T. Laliberte, "An anthropomorphic underactuated robotic hand with 15 Dofs and a single actuator," *IEEE Intl. Conf. on Robotics and Automation*, 2008.
- [6] L. Birglen, T. Laliberte, and C. Gosselin, *Underactuated Robotic Hands*. Springer Tracts in Advanced Robotics, 2008.
- [7] C. Gosselin, T. Laliberte, and T. Degoullange, "Underactuated robotic hand," in *Video Proceedings of the IEEE Intl. Conf. on Robotics and Automation*, 1998.
- [8] T. Laliberte, L. Birglen, and C. M. Gosselin, "Underactuation in robotic grasping hands," *Machine Intelligence & Robotic Control*, vol. 4, no. 3, pp. 1–11, 2002.
- [9] R. Kurtz and V. Hayward, "Dexterity measure for tendon actuated parallel mechanisms," in *IEEE Intl. Conf. on Advanced Robotics*, 1991.
- [10] A. Bicchi and D. Prattichizzo, "Analysis and optimization of tendinous actuation for biomorphically designed robotic systems," *Robotica*, vol. 18, pp. 23–31, 2000.
- [11] N. Pollard and R. Gilbert, "Tendon arrangement and muscle force requirements for humanlike force capabilities in a robotic finger," *IEEE Intl. Conf. on Robotics and Automation*, pp. 3755–3762, 2002.
- [12] J. Fu and N. Pollard, "On the importance of asymmetries in grasp quality metrics for tendon driven hands," in *IEEE-RAS Intl. Conf. on Intelligent Robots and Systems*, 2006.
- [13] C. Brown and H. Asada, "Inter-finger coordination and postural synergies in robot hands via mechanical implementation of principal components analysis," in *IEEE-RAS International Conference on Intelligent Robots and Systems*, 2007, pp. 2877–2882.
- [14] M. C. Carrozza, G. Cappiello, S. Micera, B. B. Edin, L. Beccai, and C. Cipriani, "Design of a cybernetic hand for perception and action," *Biol. Cybern.*, vol. 95, no. 6, pp. 629–644, 2006.
- [15] M. Mason and K. Salisbury, *Robot hands and the mechanics of manipulation*. MIT Press, 1985.
- [16] M. Buss, H. Hashimoto, and J. Moore, "Dextrous hand grasping force optimization," *IEEE Trans. on Robotics and Automation*, vol. 12, pp. 406–418, 1996.
- [17] L.-W. Tsai, *Robot Analysis*. John Wiley & Sons, 1999.
- [18] L. Han, J. Trinkle, and Z. Li, "Grasp analysis as linear matrix inequality problems," *IEEE Trans. on Robotics and Automation*, vol. 16, pp. 663–674, 2000.
- [19] M. Ciocarlie and P. Allen, "A design and analysis tool for underactuated compliant hands," in *IEEE-RSJ International Conference on Intelligent Robots and Systems*, 2009.
- [20] D. Prattichizzo and J. C. Trinkle, "Grasping," in *Springer Handbook of Robotics*. Springer, 2008, pp. 671–700.
- [21] A. Miller and H. Christensen, "Implementation of multi-rigid-body dynamics within a robotic grasping simulator," in *IEEE Intl. Conference on Robotics and Automation*, 2003, pp. 2262–2268.
- [22] S. Kwak, L. Blankevoort, and G. Ateshian, "A mathematical formulation for 3D quasi-static multibody models of diarthroidal joints," *Computer Meth. in Biomech. and Biomed. Eng.*, vol. 3, pp. 41–64, 2000.
- [23] A. Miller and P. K. Allen, "Graspl!: a versatile simulator for robotic grasping," *IEEE Robotics and Automation Magazine*, vol. 11, no. 4, pp. 110–122, 2004.
- [24] C. Ferrari and J. Canny, "Planning optimal grasps," in *IEEE International Conference on Robotics and Automation*, 1992, pp. 2290–2295.
- [25] M. Ciocarlie, C. Lackner, and P. Allen, "Soft finger model with adaptive contact geometry for grasping and manipulation tasks," in *Joint Eurohaptics Conference and IEEE Symp. on Haptic Interfaces*, 2007, pp. 219–224.